Phonons in Nanocrystalline ^{57}Fe

B. Fultz,[1] C. C. Ahn,[1] E. E. Alp,[2] W. Sturhahn,[2] and T. S. Toellner[2]
[1]*Division of Engineering and Applied Science, 138-78, California Institute of Technology, Pasadena, California 91125*
[2]*Advanced Photon Source, Argonne National Laboratory, Argonne, Illinois 60439*
(Received 13 March 1997)

We measured the phonon density of states (DOS) of nanocrystalline Fe by resonant inelastic nuclear γ-ray scattering. The nanophase material shows large distortions in its phonon DOS. We attribute the high energy distortion to lifetime broadening. A damped harmonic oscillator model for the phonons provides a low quality factor, Q_u, averaging about 5, but the longitudinal modes may have been broadened most. The nanocrystalline Fe also shows an enhancement in its phonon DOS at energies below 15 meV. The difference in vibrational entropy of the bulk and nanocrystalline Fe was small, owing to competing changes in the nanocrystalline phonon DOS at low and high energies. [S0031-9007(97)03708-3]

PACS numbers: 76.80.+y, 61.72.–y, 63.20.–e

Over the past decade there has been much interest in nanocrystalline materials, generally defined as materials composed of crystallites smaller than 100 nm. Unusual mechanical properties and soft magnetic properties were topics of numerous investigations on metallic nanocrystals [1]. Very recently, neutron inelastic scattering measurements have shown some differences in the phonon density of states (DOS) of nanocrystalline and bulk materials [2–6]. One such effect was an enhancement of the phonon DOS at low energies [3–7]. A broadening of the peak from the longitudinal modes in the phonon DOS was also observed and attributed to the lifetime broadening of phonons in small crystals [5,6]. Unfortunately, it was not possible to measure accurately the shape of the longitudinal peak, owing to statistical and background limitations of the neutron inelastic scattering technique.

In this Letter we show how a recently developed experimental technique, resonant inelastic nuclear γ-ray scattering [8,9], provides new information on the shape of the phonon DOS of nanocrystalline Fe. In particular, the excellent signal-to-noise ratio of the data makes it possible to examine quantitatively the high energy tail of the phonon DOS in small samples. In our resonant inelastic nuclear γ-ray scattering measurements, 14.41 keV γ rays were directed onto a foil specimen, and 6.4 keV conversion x-ray radiations from the specimen were detected. This scattering is incoherent, so the data provide information on the velocity-velocity correlation function of individual ^{57}Fe nuclei. The experiments were performed at the undulator beamline 3-ID at the Advanced Photon Source. A high-heat-load monochromator, which consists of two symmetric silicon (1 1 1) reflections in a nondispersive setting, and a high-resolution, nested monochromator, as described previously [10], were used to provide the 14.413 keV radiation onto the specimen. The high-resolution monochromator operates with asymmetric silicon (4 2 2) and symmetric silicon (10 6 4) reflections and produces a constant energy bandwidth of 5.5 meV over the tuning range. The energy of the incident radiation was tuned by rotating the (10 6 4) channel-cut crystal in steps of 2 meV. The photons were incident on the sample at 5×10^9 Hz in a 0.5×2 mm^2 beam. An avalanche photo diode with an active area of 2 cm^2 was mounted 3 mm above the specimen for the detection of the emitted Fe-K fluorescence radiation. To eliminate the unwanted electronic contribution to the fluorescence, counting began 30 ns after the arrival of the synchrotron radiation flash. The detector noise was less than 0.03 Hz. All measurements were performed at room temperature. A foil of cold-rolled bulk ^{57}Fe was used for calibration and comparison with the nanocrystalline material.

The sample of nanocrystalline ^{57}Fe was prepared by the technique of ballistic consolidation [11]. About 34 mg of ^{57}Fe (95% isotopically enriched) was evaporated by electrical resistance heating into a gas of N_2 containing 10 vol % H_2 at a pressure of 3.5 Torr. Some of the ^{57}Fe crystallites that condensed in the flowing gas were entrained as aerosol particles in a gas stream that was drawn through a nozzle of 1 cm diameter. Particle velocities of 20 m/s were achieved by establishing a pressure of 1000 mT on the downstream side of the nozzle. This gas was directed against a thin kapton substrate, where a film of about 4 mg of ^{57}Fe was deposited.

An x-ray diffraction pattern from the nanocrystalline ^{57}Fe film is shown in Fig. 1(a). The main diffraction peaks are indexed as bcc Fe. We determined the lattice parameter of the bcc phase to be 2.8679 ± 0.0005 Å, which is close to the lattice parameter of 2.8664 Å of pure Fe. Also visible are broad diffraction features attributable to a thin oxide layer around the surfaces of the Fe crystallites. Although the oxide may be amorphous, after six months of exposure to air the sample oxidation was more extensive (although not complete), and the oxide was identified as either nanocrystalline maghemite or magnetite. We estimated the particle sizes and strain distribution in the bcc phase from the widths of the (110)

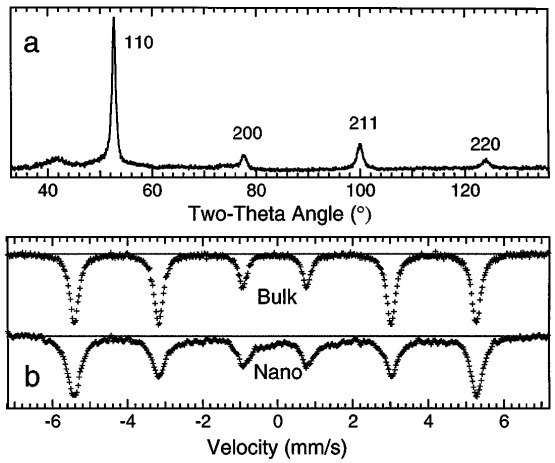

FIG. 1. (a) X-ray diffraction pattern from ballistically consolidated nanocrystalline ^{57}Fe. Main peaks are indexed as bcc Fe. Kapton substrate contributes to diffraction intensity at lower angles, but intensity around 74° is from oxide. (b) Top: transmission Mössbauer spectrum of bulk foil from natural Fe. Bottom: spectrum from ballistically consolidated nanocrystals of natural Fe.

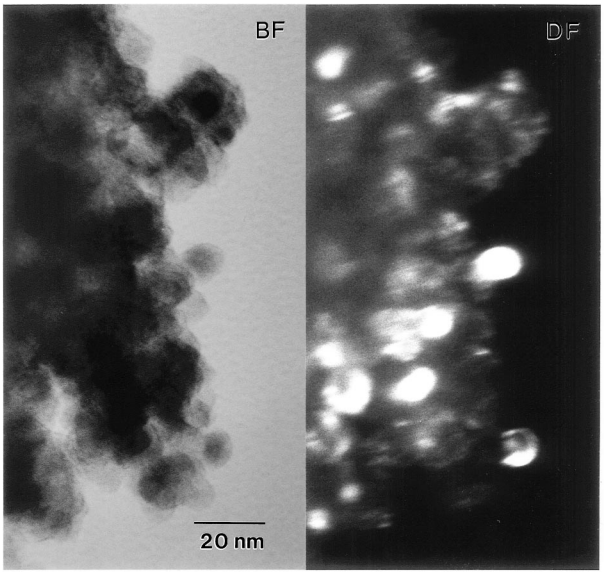

FIG. 2. Transmission electron micrographs of ballistically consolidated nanocrystals of ^{57}Fe. Left: bright field. Right: dark field image from (110) bcc Fe diffraction.

and (220) diffractions [12], obtaining a small crystalline size, (10 ± 1) nm, and a root-mean-squared strain of $(0.18 \pm 0.03)\%$.

Figure 1(b) shows a conventional transmission Mössbauer spectrum from a similar sample of nanocrystalline natural Fe prepared by ballistic consolidation. Compared to the Mössbauer spectrum from bulk Fe, there is some broadening of the sextet of peaks in the nanocrystalline film. Such broadening has been attributed previously to Fe atoms at grain boundaries [13] or free surfaces [14]. There is also a small amount of paramagnetic Fe evident in the spectrum. Although it is not practical to assign the paramagnetic spectrum to a crystal structure, the intensity is within the range expected of iron oxides. Finally, the Mössbauer spectrum also contains a weak and broad contribution from -5 to $+5$ mm/s, perhaps originating with Fe atoms in irregular local environments of grain boundaries [15] or surfaces, for which magnetic relaxation may occur at room temperature [14].

Transmission electron microscopy was performed on several samples of natural Fe and one sample of ^{57}Fe prepared by ballistic consolidation. Figure 2 shows that the crystallites are distinct, with sizes around 10 nm and with the uniformity expected from the gas consolidation method [1]. The images allow for only thin disordered regions between crystallites and thin surface oxides. The state of agglomeration and consolidation was controlled by the conditions of ballistic consolidation to provide some internal porosity as seen in the bright field image.

Typical resonant inelastic nuclear γ-ray scattering spectra are presented in Fig. 3. An important point about the experimental data is the negligible background. Data points away from the Mössbauer resonance (e.g., at energies greater than ± 90 meV) averaged only two counts on the scale of Fig. 3. The resonant inelastic nuclear γ-ray scattering spectrum from the nanocrystalline material in Fig. 3 shows a tail above 40 meV that extends beyond that of the bulk bcc Fe, and also shows an enhanced scattering at low energies below 15 meV.

Analysis of the resonant inelastic nuclear γ-ray scattering spectra to obtain phonon DOS curves proceeded in the same way as for incoherent inelastic neutron scattering. The resulting DOS curve is technically a partial phonon DOS from ^{57}Fe alone, but this is nearly equivalent to the total phonon DOS of our specimens. The elastic

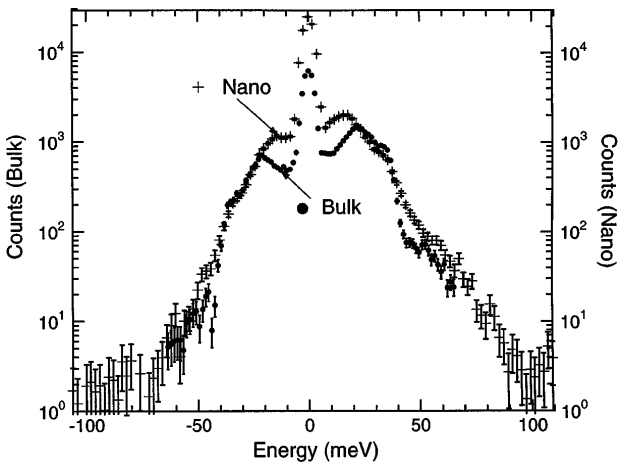

FIG. 3. Experimental resonant inelastic nuclear γ-ray scattering spectra from bulk ^{57}Fe foil and ballistically consolidated nanocrystalline ^{57}Fe. Data are shown with equal intensity at 25 meV.

peaks were modeled as a sum of two Gaussian peaks, and subtracted from the spectrum. The resulting inelastic scattering was treated with the conventional multiphonon expansion [16,17]. A calculation of the phonon DOS of bcc Fe, using the Born–von Kármán model of lattice dynamics with force constants obtained from experimental phonon dispersion curves [18], is shown at the top of Fig. 4(a), labeled "Fe DOS." From this phonon DOS curve it is straightforward to calculate the multiphonon scattering at 300 K with a momentum transfer vector Q of the 14.41 keV γ rays (7.3 Å^{-1}). For this Q, T, and DOS of bcc ^{57}Fe, the multiphonon scattering (sum of 2-, 3-, 4-, 5-phonon scatterings) is in a fixed ratio to the total inelastic scattering (sum of 1, 2, 3, 4, 5-phonon scatterings). After convolving these calculated scattering functions $S(Q, E)$ with a Gaussian resolution function of FWHM = 5.0 meV, the total inelastic scattering was scaled in amplitude to fit the experimental inelastic scattering data. The multiphonon scattering was scaled by the same factor, and subtracted from the experimental data. The result is the experimental one-phonon scattering. This one-phonon scattering can be converted into a phonon DOS by multiplying by the thermal correction factor $f(E)$:

$$f(E) = E[1 - \exp(-E/kT)]. \quad (1)$$

The only difficulty with the procedure just described is knowing the phonon DOS to use for calculating the multiphonon scattering. While this is not a problem for bulk bcc Fe, the phonon DOS is not known *a priori* for the nanocrystalline material. In one approach we used an iterative procedure. We started by assuming the multiphonon scattering of bcc Fe, and extracted a phonon DOS curve from the experimental data. This first generation DOS curve was then used to calculate the multiphonon scattering for the second iteration. There was essentially no difference for the phonon DOS obtained in the first and second iterations for the bulk Fe sample, and relatively little change for the phonon DOS from the nanocrystalline material. The method of Sturhahn *et al.* [8] was also used to obtain phonon DOS curves, and results of the two methods were essentially identical.

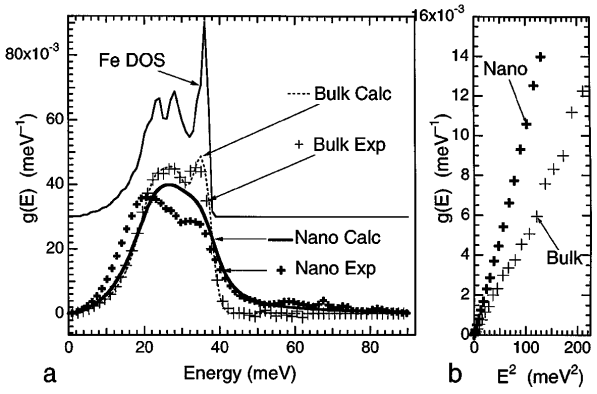

FIG. 4. (a) Top: phonon DOS of bulk bcc Fe, calculated with force constants from inelastic neutron scattering [18]. Bottom: crosses are phonon DOS curves extracted from experimental data of Fig. 4. Solid curves are calculated as described in text. (b) Enlargement of low energy part of the experimental phonon DOS curves of Fig. 4(a).

The experimental phonon DOS curves obtained after the second iteration are shown in Fig. 4(a) as "Bulk Exp" and "Nano Exp." They are overlaid with two calculated curves. The curve labeled "Bulk Calc" is the phonon DOS from bcc Fe [labeled Fe DOS in Fig. 4(a)] after convolution with a Gaussian instrument function of 5.0 meV resolution. The fit to the experimental data is excellent, even though the only adjustable parameter was the normalization to unit area.

The curve labeled "Nano Calc" was also obtained from the phonon DOS of bcc Fe, but with the assumption of lifetime broadening of the phonons. Each intensity at energy E' of the curve Fe DOS was convoluted with the characteristic spectrum of a damped harmonic oscillator:

$$D_{E'}(E) = \frac{1}{\pi Q_u E'} \frac{1}{(E'/E - E/E')^2 + 1/Q_u^2} \quad (2)$$

The only free parameter in fitting the phonon DOS from the nanocrystalline material was the value of the quality factor of the oscillator Q_u, which was assumed to be the same for all phonons. The curve Nano Calc in Fig. 4(a) was obtained with a value of $Q_u = 5$, after convolution with the same instrument resolution function used for the bulk Fe data (Gaussian function of FWHM = 5.0 meV). Many features of the phonon DOS from the nanocrystalline Fe are represented well by this assumption of a damped harmonic oscillator. The shape of the high energy tail above the longitudinal peak is modeled particularly well. It is possible, however, to obtain better agreement with the kink in the experimental data at 30 meV by assuming that the transverse modes are broadened less than the longitudinal modes.

The lifetime broadening can be understood by considering the number of oscillation cycles available to a phonon wave packet as it traverses a small crystallite. In a 10 nm crystallite, half of the atoms are within about 1 nm from the surface. The present value of $Q_u = 5$ is much lower than from nanocrystalline material in consolidated form [5,6], however. Previous results from consolidated fcc nanocrystals of 10 nm indicate a Q_u in the range of 15–30 [6]. We believe our low value of Q_u originates with the open nature of the microstructure shown in Fig. 2, and perhaps from effects of surface oxide. We hypothesize that the interfaces and free surfaces in our material may be especially effective in damping crystal vibrations, at least those of longitudinal polarization. We doubt that damping could be caused by interstitial contamination in the metal by C or N atoms; the small change in x-ray lattice parameter compared to that of bulk bcc Fe indicates a concentration of C or N of less than 0.2 at.% [19]. It might be argued that some damping could originate with internal

stresses. For small particles there is a large thermodynamic driving force to reduce surface area, so the atoms bounding the regions of contact between two small crystallites could be subject to severe stresses. These stresses will be propagated into the nanocrystallites [20], and may scatter phonons by anharmonic interactions. The measured strain distribution is smaller than in ball-milled Fe, however, which shows much less phonon broadening [5].

There remain two discrepancies between the curves Nano Exp and Nano Calc that we believe are significant. For energies below about 15 meV, Fig. 4(b) shows that the DOS from the ballistically consolidated nanocrystals lies above the DOS from the bulk Fe sample by a factor of about 2 (there may be some uncertainty at energies below about 4 meV, owing to how we subtracted the elastic Mössbauer peak from the data). Such low energy modes have been reported previously [4–7]. Although their origin is not fully understood, they are consistent with a high density of elastic discontinuities in the material [21,22]. It is interesting that the experimental data shown in Fig. 4(b) are approximately quadratic in energy, although with different constants of proportionality. Perhaps the average velocity of sound is smaller in the nanocrystalline material by a factor of $\sqrt[3]{2} = 1.26$. The second discrepancy of note is an enhanced experimental intensity in the energy range 55–75 meV. Although the signal is weak, we suggest it could originate with Fe atoms that are bonded covalently to O atoms. High frequency vibrations of O atoms would cause a small response of neighboring Fe atoms at the same frequency.

A large entropy has been proposed as a reason for the thermal stability of nanocrystalline materials at moderate temperatures [23,24]. We define $\Delta S_{\mathrm{vib}} = S_{\mathrm{vib}}^{\mathrm{nan}} - S_{\mathrm{vib}}^{\mathrm{blk}}$ as the difference in vibrational entropy of the nanocrystalline and the bulk Fe. At high temperatures this difference in vibrational entropy depends in a straightforward way on the difference in the vibrational DOS of the two phases, $g^{\mathrm{nan}}(E) - g^{\mathrm{blk}}(E)$ [3,5]:

$$\Delta S_{\mathrm{vib}} = -3k_B \int_0^\infty [g^{\mathrm{nan}}(E) - g^{\mathrm{blk}}(E)] \ln(E)\, dE\,, \quad (3)$$

where the difference avoids problems with the dimensions of the argument of the logarithm. Using the vibrational DOS shown in Fig. 4(a), for high temperature we find $\Delta S_{\mathrm{vib}} = 0.01 \pm 0.02 k_B/\mathrm{atom}$. Other nanocrystalline materials that had a significant enhancement of their phonon DOS at low energies have had vibrational entropies up to $0.2 k_B/\mathrm{atom}$ larger than their bulk counterparts [3,5,6]. In the present alloy, surprisingly, the large lifetime broadening of the DOS from the nanocrystalline material largely cancels the effects from the enhancement of the phonon DOS at low energies. It is unlikely that the thermodynamic stability of our nanocrystalline Fe is affected much by vibrational entropy.

The work at Caltech was supported by the U.S. National Science Foundation under Contract No. DMR-9415331, and the work at Argonne was supported by the U.S. Department of Energy under Contract No. W-31-109-EN-38.

[1] See, for example, H. Gleiter, Prog. Mater. Sci. **33**, 223 (1989); R. W. Siegel, Phys. Today **46**, 64 (1993).
[2] K. Suzuki and K. Sumiyama, Mater. Trans. JIM **36**, 188 (1995).
[3] B. Fultz, L. Anthony, L. J. Nagel, R. M. Nicklow, and S. Spooner, Phys. Rev. B **52**, 3315 (1995).
[4] J. Trampenau, K. Bauszuz, W. Petry, and U. Herr, Nanostruct. Mater. **6**, 551 (1995).
[5] B. Fultz, J. L. Robertson, T. A. Stephens, L. J. Nagel, and S. Spooner, J. Appl. Phys. **79**, 8318 (1996).
[6] H. N. Frase, L. J. Nagel, J. L. Robertson, and B. Fultz, Philos. Mag. B **75**, 335 (1997).
[7] D. Wolf, J. Wang, S. R. Phillpot, and H. Gleiter, Phys. Rev. Lett. **74**, 4686 (1995).
[8] W. Sturhahn *et al.*, Phys. Rev. Lett. **74**, 3832 (1995).
[9] M. Seto, Y. Yoda, S. Kikuta, X. Zhang, and M. Ando, Phys. Rev. Lett. **74**, 3828 (1995).
[10] T. M. Mooney, T. S. Toellner, W. Sturhahn, E. E. Alp, and S. D. Shastri, Nucl. Instrum. Methods Phys. Res., Sect. A **347**, 348 (1994).
[11] J. S. Reid, R. A. Brain, and C. C. Ahn, *Proceedings of the 12th International VLSI Multilevel Interconnect Conference*, edited by T. E. Wade (Santa Clara, CA, 1995), p. 545.
[12] H. P. Klug and L. E. Alexander, *X-Ray Diffraction Procedures* (Wiley-Interscience, New York, 1974), pp. 656 and 664.
[13] U. Herr, J. Jing, R. Birringer, U. Gonser, and H. Gleiter, Appl. Phys. Lett. **50**, 472 (1987).
[14] R. J. Pollard and J. Chadwick, Hyperfine Interact. **94**, 2245 (1994).
[15] B. Fultz, H. Kuwano, and H. Ouyang, J. Appl. Phys. **77**, 3458 (1995).
[16] G. L. Squires, *Introduction to the Theory of Thermal Neutron Scattering* (Cambridge Univ. Press, Cambridge, 1979), pp. 54–58.
[17] V. F. Sears, E. C. Svensson, and B. M. Powell, Can. J. Phys. **73**, 726 (1995).
[18] V. J. Minkiewicz, G. Shirane, and R. Nathans, Phys. Rev. **162**, 528 (1967).
[19] L. Cheng, A. Bottger, Th. H. de Keijser, and E. J. Mittemeijer, Scr. Metall. Mater. **24**, 509 (1990).
[20] H. L. Zhu and R. S. Averback, Philos. Mag. Lett. **73**, 27 (1996).
[21] A. Tamura and T. Ichinokawa, J. Phys. C **16**, 4779 (1983).
[22] S. Trapp, C. T. Limbach, U. Gonser, S. J. Campbell, and H. Gleiter, Phys. Rev. Lett. **75**, 3760 (1995).
[23] H. J. Fecht, Phys. Rev. Lett. **65**, 610 (1990).
[24] M. Wagner, Acta Metall. Mater. **40**, 957 (1992).